

Airfoil Pressure Measurements During a Blade Vortex Interaction and a Comparison with Theory

J. Straus,* P. Renzoni,† and R. E. Mayle‡
Rensselaer Polytechnic Institute, Troy, New York

A two-dimensional, airfoil-vortex interaction experiment was conducted to obtain the aerodynamic behavior of the airfoil during a parallel interaction. The vortex was created by pitching a second airfoil placed upstream and parallel to an instrumented test airfoil. Hot-wire anemometer measurements were taken to determine the vortex velocity distribution. The interaction tests were conducted for a counterclockwise vortex passing above a symmetrical airfoil at zero angle of attack. Pressure transducers located inside the test airfoil measured steady and unsteady airfoil pressure distributions. Time histories of the lift, drag, and moment coefficients were determined from the measured pressure distributions. These results are compared to an analytical study using an unsteady, discrete-vortex, potential-flow theory. The comparison leads one to conclude that under certain conditions the airfoil separated during the interaction.

Nomenclature

C_D	= coefficient of drag, $2D/pU_\infty^2 c$
C_L	= coefficient of lift, $2L/pU_\infty^2 c$
C_M	= coefficient of moment, $2M/pU_\infty^2 c$
C_p	= coefficient of pressure = $2(P - P_\infty)/\rho U^2$
C_{pU}	= coefficient of pressure, upper surface
C_{pL}	= coefficient of pressure, lower surface
c	= blade chord
c_1	= vortex generator chord
h_0	= plunging amplitude
K_{RF}	= reduced frequency, $\omega c_1/2U_\infty$
t	= time
U_∞	= freestream velocity
v_0	= tangential velocity
x	= chordwise position on blade
y/c_1	= nondimensional position wrt vortex center
$(y/c)_0$	= initial position of vortex wrt test airfoil
α	= angle of attack
Γ	= vortex circulation
Ω	= angular velocity
ω	= frequency of airfoil oscillation

Introduction

IT is generally recognized that blade-vortex interactions lead to severe impulsive aerodynamic loadings and noise problems in rotorcraft. Figure 1a shows how a rotor blade can intersect its own trailing-tip vortex under certain operating conditions. These interactions usually occur in helicopter forward flight with a powered descent and occur such that the blade and vortex intersect at a variety of angles. Two important interaction extremes occur when the vortex is either perpendicular (Fig. 1b) or parallel (Fig. 1c) to the airfoil. A perpendicular interaction more likely affects only a small spanwise portion of the airfoil, whereas a parallel interaction, such as that shown imminent in Fig. 1a, affects most of the airfoil. In addition, Widnall¹ and Nakamura² found that the greatest effect on noise occurs when the vortex is directed parallel to the airfoil's leading edge. Therefore, it is suspected that detailed measurements for a parallel blade-vortex interaction are more crucial to understanding the associated airload and noise problems.

Experiments having a streamwise directed vortex passing perpendicular, or nearly so, to an airfoil (Fig. 1b) are rather simple to conduct, since the vortex is easily produced by using an angled wing tip placed upstream of the test airfoil. The situation is nominally steady, and the resulting flows are three-dimensional and difficult to analyze theoretically. On the other hand, experiments with parallel blade-vortex interaction having the vortex directed across the flow (Fig. 2c) are unsteady, difficult to conduct, but easier to analyze. This paper describes experiments on parallel blade-vortex interactions, their results, and comparisons to an inviscid theory.

There have been numerous experiments conducted on blade-vortex interactions. However, most of the experiments have dealt with noise measurements in helicopter rotor flight configurations. The reader interested in this aspect of the problem is referred to Refs. 3–12. The work described in Refs. 3–8 concerns experiments in wind tunnels using helicopter rotor configurations, and those described by Brotherhood⁹ and Schmitz et al.¹⁰ present additional results from full-scale testing. Furthermore, Refs. 3–5 examine the surface pressure vari-

Presented as Paper 88-0669 at the AIAA 26th Aerospace Sciences Meeting, Reno, NV, Jan. 11–14, 1988; received Feb. 8, 1988; revision received Sept. 12, 1988. This paper is declared a work of the U.S. Government and is not subject to copyright protection in the United States.

*Graduate Student. Mechanical and Aeronautical Engineering Department. Member AIAA.

†Graduate Student. Mechanical and Aeronautical Engineering Department; currently Research Scientist, CIRA, Italy. Member AIAA.

‡Professor, Department of Mechanical Engineering, Aeronautical Engineering, and Mechanics. Member AIAA.

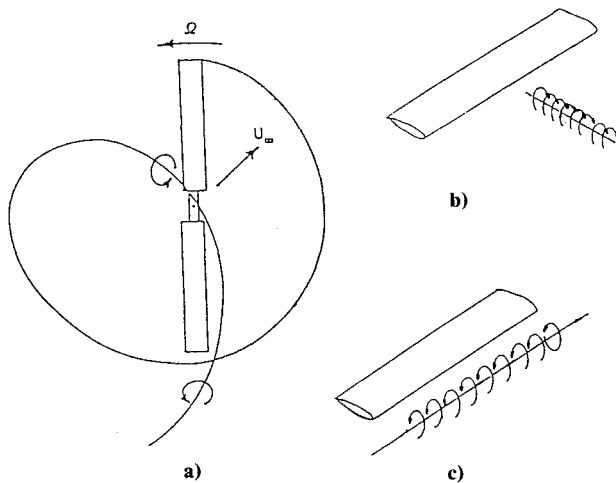


Fig. 1 Airfoil interactions with a concentrated vortex: a) rotor-trailed vortex filament; b) perpendicular interaction; c) parallel interaction.

ations over an airfoil, and Refs. 5–10 deal with farfield noise measurements. A comprehensive survey of the theoretical and experimental work on helicopter noise, including that from blade-vortex interactions, is presented by George¹¹ and Schmitz and Yu.¹² However, since the work discussed in these references is more concerned with noise, the authors generally fail to examine the fundamental fluid-mechanic problem related to an unsteady blade-vortex interaction.

Other experiments have considered in greater detail the aerodynamics of the perpendicular blade-vortex interaction problem. Ham^{13,14} studied such effects by means of an instrumented rotating blade interacting with a streamwise vortex as well as with a stationary test airfoil. Neuwerth and Muller¹⁵ investigated a second type of normal interaction orientation such that the vortex axis was parallel to the rotor axis. McAlister and Tung¹⁶ used the hydrogen bubble technique in a water tunnel to aid in the visualization of normal incidence interactions. They concluded that the presence of the vortex caused premature stalling of the test airfoil, regardless of the side on which the vortex passes. Wilson and Seath¹⁷ observed that such interactions can cause a spanwise drift of the vortex while passing over the airfoil. However, both sets of authors show that the spanwise effects are rather local.

The effects of two-dimensional, parallel blade-vortex interactions on both noise and aerodynamics have only been considered by a few experimental investigators. Surendraiah¹⁸ and Caradonna et al.¹⁹ investigated parallel blade-vortex interactions for airfoils in rotor configurations. Recent investigations by Ziada and Rockwell,²⁰ Seath et al.,²¹ and Booth and Yu^{22–25} provided flow visualization. The experiments of Booth and Yu were conducted at a chord Reynolds number of 85,000. In addition, temporal pressure measurements were made around the leading edge of the airfoil during the blade-vortex interaction. Their results showed two “lobes” of pressure perturbations near the leading edge during the interaction: one on each side of the airfoil. The lift also showed large fluctuations, and it was concluded that this was the source of “blade slap.” A more complete set of airfoil pressure measurements during vortex interactions was provided by Seath et al.²¹ Their investigations included measurements for parallel interactions with flows for incident Reynolds numbers ranging from 100,000 to 200,000 and, in general, substantiated the results of Booth and Yu.^{22–25} In addition, they showed that either a decrease in the interaction distance, an increase in the vortex strength, or a decrease in the incident velocity caused a greater interaction effect. However, since their pressure measurements were overdamped by the long tube connecting the transducer to the tap, the accuracy of their results is somewhat questionable.

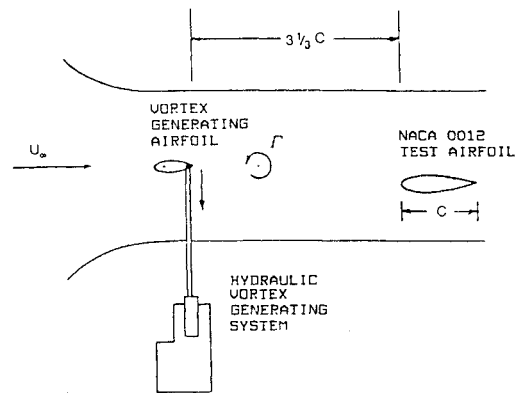


Fig. 2 Schematic of test section and blade-vortex interaction setup.

Shock-tube experiments have been conducted by Meier and Timm.^{26,27} The two-dimensional vortices were generated by different vortex-shedding cylinders or by an airfoil placed upstream in the starting flow. Both vortex trajectories and pressure measurements made in high-speed blade-vortex interactions are reported. Test Mach numbers varied from 0.2 to 0.8. Typical Reynolds numbers presented were of the order of 300,000. Interferometry measurements showed the presence of a secondary vortex for close interactions, possibly originating from a formed separation bubble.

The object of the present experiments was to study the fundamental problem of two-dimensional blade-vortex interactions and compare the results with an inviscid, two-dimensional analysis by Renzoni.²⁸ The experiment was similar to those of Seath et al.²¹ and Booth and Yu^{22–25} in that a parallel, force-free vortex was produced by a second upstream airfoil. The main difference was that the experiments were conducted with an airfoil model that was large enough to facilitate future unsteady boundary-layer measurements.

Experimental Facility and Apparatus

The blade-vortex interaction experiments were conducted in a 1.2×1.8 m closed-circuit wind tunnel at a mainstream velocity of 12.2 m/s. A schematic of the test configuration is shown in Fig. 2. A NACA 0012 test airfoil with a 46-cm chord and 180-cm span was placed approximately 150 cm downstream of a NACA 0018 vortex-generating airfoil having a 25-cm chord and 152-cm span. When the upstream airfoil was suddenly pitched, a single, two-dimensional cast-off vortex was generated that convected downstream, parallel to the test airfoil. The response time of the pitching system is crucial to producing a single cast-off vortex. It is required to keep the time it takes to complete the pitching motion less than the time it takes the air to travel one chord of the pitching airfoil. For the present test situation, this threshold time is about 21 ms. The actual time required to pitch the airfoil was about 15 ms.

A Moog hydraulic system was used to pitch the airfoil about its center of mass. A separate linear servomotor was used for each side of the vortex-generating airfoil. Each servomotor was equipped with a linear voltage displacement transducer that allowed the feedback control system to reliably reproduce the pitching motion. This was necessary because the unsteady and turbulent nature of the flow requires that many measurements at the same conditions be obtained and the results ensemble averaged. A function generator having a square-wave output was used to set the amplitude of the pitch angle. A manual trigger of the function generator resulted in a single pitch of the airfoil.

The Reynolds number of the vortex-generating airfoil for these experiments was nominally 210,000. The NACA 0018 profile was specifically chosen so that the airfoil could operate at this Reynolds number without separating over a large variation in incident angles of attack. The airfoil was made mostly

of styrofoam and had a fiberglass-epoxy surface. Its lightness, considering its size, was essential to the system's quick response. Two 15.2-cm wide graphite sheets having ± 45 and 0-deg fiber orientation were bonded on both sides of the airfoil between the foam and fiberglass along the span of the airfoil to provide bending and torsional strength. Those interested in further details regarding the hydraulic system and the vortex-generating airfoil construction are referred to Bergman.²⁹

The test airfoil was constructed of mahogany and contains a central, removable instrumented section, as shown in Fig. 3. It spanned the complete width of the tunnel. The NACA 0012 profile was reproduced to within 0.8 mm in the chordwise direction and to within 2 mm in the spanwise direction. It was finished with a light protective coat of polyurethane varnish. The instrumented section had 21 pressure taps positioned along the chord on one side of the airfoil and three taps on the other side. More taps were located near the leading edge, where the largest pressure gradients were expected. Detailed pressure measurements on both sides of the airfoil were obtained by inverting the airfoil in the tunnel. Table 1 contains the pressure tap locations.

The 24 taps were connected through two miniature, air-driven Scanivalves to two high-resolution pressure transducers. The differential pressure transducers (Kulite XCS-093-5D) were equipped with a temperature-compensation circuit and separate output signal amplifiers having a gain of about 10,000. The airfoil pressure measurements were referenced to the static pressure of the incident flow. This was accomplished by attaching the reference tap on each transducer to two small tanks inside the airfoil that were sufficiently large to maintain a nearly constant pressure during the interaction time. These tanks were in turn connected to the static tap of the incident flow Pitot-static probe. To minimize the response time of the pressure measurement system and increase the signal-to-noise ratio, all of the pressure measurement apparatus and electronics were placed in the airfoil. The time response of the system was about 0.5 ms.

Velocity measurements in both the mainstream and boundary layer of the test airfoil were made using a TSI hot-wire probe and anemometer system. Velocity profiles were obtained using a traverse mechanism attached to the upper tunnel wall. To measure the unsteady component of the flow caused by the vortex, the anemometer's output was biased using the steady mean flow voltage and then amplified.

Since the flow was unsteady and turbulent, all measurements were ensemble-averaged to provide the corresponding time-varying mean value. This was accomplished by using a Nicolet digital oscilloscope triggered by the motion of the vortex-generating airfoil and simply summing the data acquired from pitching the airfoil many times. An ensemble average of 10–20 data sequences was sufficient to provide an ac-

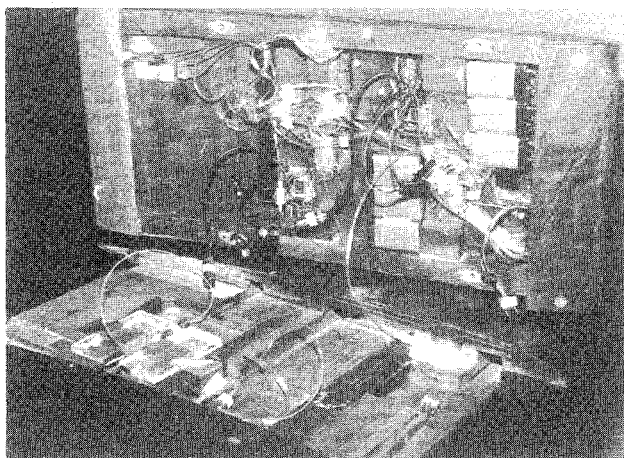


Fig. 3 Instrumented central portion of test airfoil.

Table 1 Pressure tap locations

Tap no.	x/c	Tap no.	x/c
1	0	11	0.17
2	0.003	12	0.20
1L	Reference	13	0.25
3	0.01	14	0.30
4	0.02	15	0.40
5	0.03	16	0.50
6	0.045	17	0.60
7	0.06	18	0.70
8	0.08	19	Reference
9	0.10	20	0.90
2L	0.10 Lower	3L	0.90 Lower
10	0.13	21	0.97

curate time-varying mean value. These data were stored on bubble memory in the scope and eventually transferred to a microcomputer for further analysis. A schematic of the complete experimental system is shown in Fig. 4. The reader interested in further details regarding the apparatus and procedure is referred to Straus.³⁰

Theory

Although details of the theoretical work will not be presented, a brief description is warranted. A generalized, two-dimensional, potential-flow theory for the interaction of discrete force-free vortices with a Joukowski airfoil in unsteady motion was developed.²⁸ The analysis allows for the airfoil to move either steadily or unsteadily through a fluid imbedded with vortices and allows for a freely convected wake. The solution is obtained through the well-known methods of conformal mapping and the Joukowski transformation. A calculation is made step by step in time and the motion of the vortices relative to the airfoil computed. At every time step, the vorticity that is shed into the wake is represented by a newly formed discrete vortex near the trailing edge. Its strength is determined both its position and the Kutta condition. The pressure at any point in the flow is determined by the unsteady Bernoulli equation. The forces and moments on the airfoil at any time step are calculated from either a numerical integration of the pressure distribution over the airfoil or the unsteady Blasius theorem. Although the theory is particularly suitable for arbitrary transient problems, it can also be applied to periodic motions.

Results of this discrete-vortex analysis were compared to the linear theories of Theodorsen,³¹ Sears,³² and Fung.³³ Figure 5 presents the comparison between the lift obtained using the discrete-vortex method and Theodorsen for a flat plate plunging sinusoidally at a reduced frequency of unity and at an amplitude of 2% of chord. The comparison is shown for the third period of oscillation where 40 time steps per period were used.

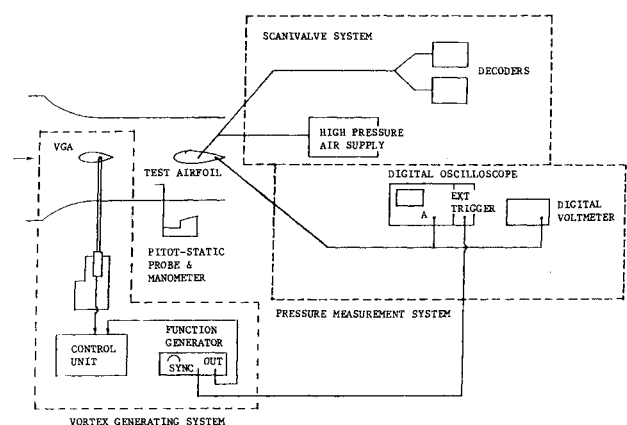


Fig. 4 Blade-vortex experimental system schematic.

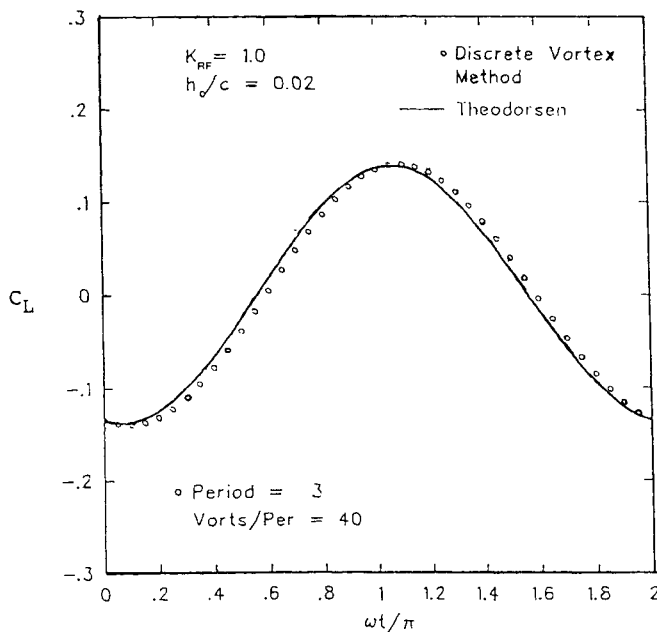


Fig. 5 Circulatory lift coefficient comparison, $h_0/c_1 = 0.02$.

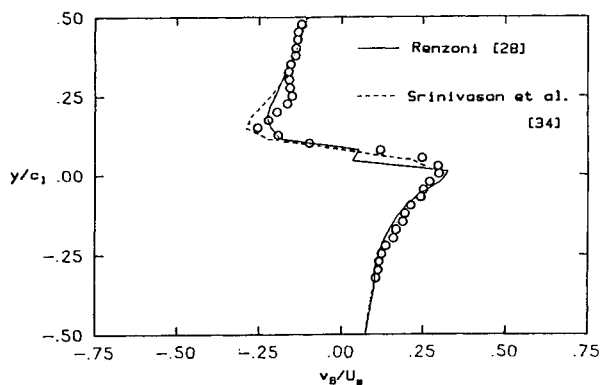


Fig. 6 Measured and calculated velocity distributions in castoff vortex.

The calculation required 30 s of cpu time on an IBM 3081 D, which is typical. As seen, a good agreement is obtained in both phase and amplitude even after only three cycles. Similar results are found in the comparisons with Sears' and Fung's work as long as the amplitudes remain small (see Ref. 28).

The comparisons with the present experimental results were somewhat more difficult to obtain and actually involved a two-step process. Since the vortex-generating airfoil was only slightly more than three chords upstream, the effect of it on the flow and the form of the "castoff wake" had to be determined. This was done by using the result of the discrete-vortex method for the upstream airfoil with an experimentally determined pitch schedule. Once the lift on the pitched airfoil became nearly constant, but before the wake of vortices reached the position of the test airfoil, the upstream airfoil was replaced by the bound vortex. The calculation was then continued using a finite cluster of force-free, discrete vortices to represent the castoff vortex and a bound vortex at the position of the vortex-generating airfoil. An 11.5% Joukowski airfoil was also used to represent the NACA 0012 test airfoil. Past studies have shown this to be quite acceptable. Those who are interested in the details of these calculations and procedure are referred to Ref. 28.

Results

To assess the character and strength of the castoff vortex, unsteady velocity measurements were made at a position 25

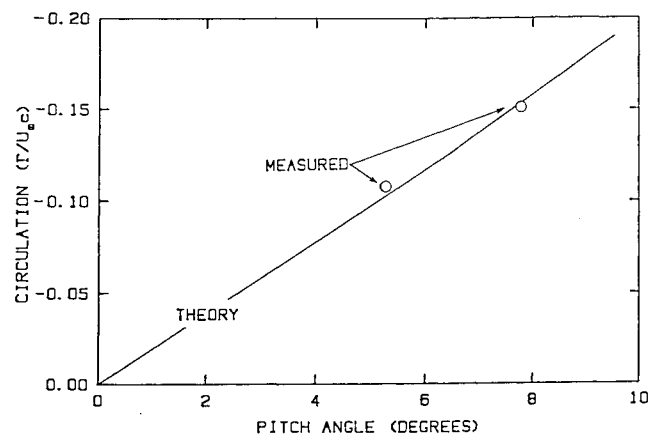


Fig. 7 Castoff vortex strength dependence on the final pitch angle of the vortex-generating airfoil.

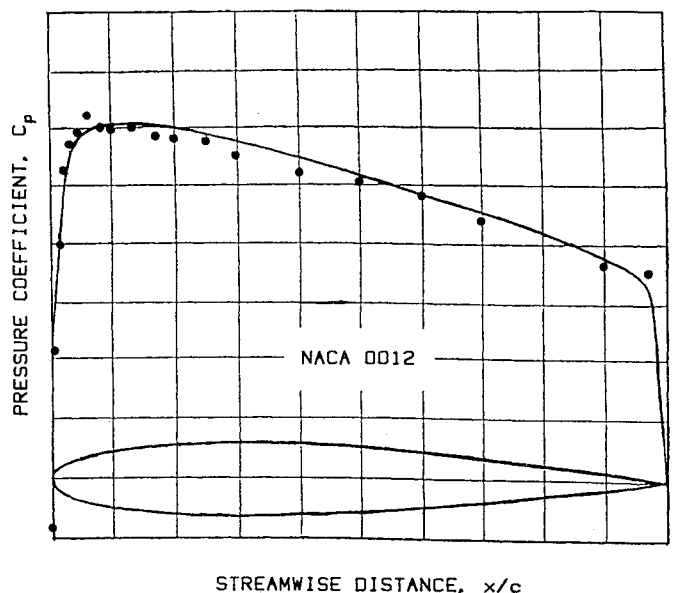


Fig. 8 Measured steady-state pressure distributions.

cm upstream of the test airfoil's leading-edge location, but without the airfoil in place. By taking measurements at different distances across the flow, the velocity component of the mean flow caused by the vortex imbedded in the flow could be determined. The distribution of this velocity component at midspan and for a downward 7.8-deg pitch of the upstream airfoil is shown in Fig. 6. In addition, the velocity distribution from the discrete-vortex analysis and a correlation by Srinivasan et al.³⁴ are shown. The horizontal axis represents the difference between the measured and freestream tunnel velocity nondimensionalized with the freestream velocity. The ordinate is the height relative to the trailing edge of the generating airfoil nondimensionalized with the airfoil's chord. Clearly, the suddenly pitched airfoil produced a tightly rolled-up vortex sheet that agrees very well with theory. The discrepancy is attributed to an incomplete diffusion of the "rolled-up" vortex sheet, which actually forms the castoff vortex. Particularly important to modeling an actual blade-vortex interaction, however, is the result that the vortex "core" is about one-tenth of a chord in diameter. This is characteristic of that found in actual helicopter blade-vortex interactions. Velocity profiles measured one chord to each side of the midspan plane indicated that the vortex was two-dimensional within the central instrumented portion of the test airfoil. In Fig. 7, a comparison is made between the measured castoff

vortex circulation for different pitch angles to that predicted by the discrete-vortex method. Again, the result is excellent.

Steady-state pressure measurements for the test airfoil without the vortex-generating airfoil in place are shown in Fig. 8. The results are plotted as C_p against a dimensionless chordwise distance and compared to those obtained by NACA. With the exception of a few points, the present data agree well. The discrepancies are attributed to the small differences in the airfoil's contour.

The C_p time histories for 10, 25, 50, and 70% chord locations on both sides of the airfoil are shown in Figs. 9 and 10. In these figures, the abscissa is a dimensionless time starting when the upstream airfoil was pitched. The position of the test airfoil in this coordinate is indicated in the figures as falling roughly between $U_\infty t/c = 3$ and 4. These results correspond to an interaction where a vortex with a counterclockwise circulation of $\Gamma/Uc = -0.15$ passed one-quarter chord above the test airfoil. The results are also compared to the discrete-vortex interaction theory. The agreement between the data and the theory is quite good over most of the airfoil. In the leading-edge region the model overestimates the pressures during the interaction but still maintains a similar behavior.

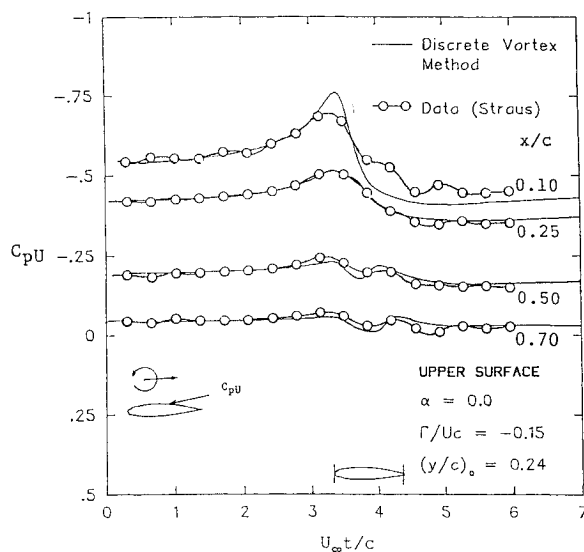


Fig. 9 Measurements of pressure-time history for upper surface and comparisons with theory, $\Gamma/Uc = -0.15$.

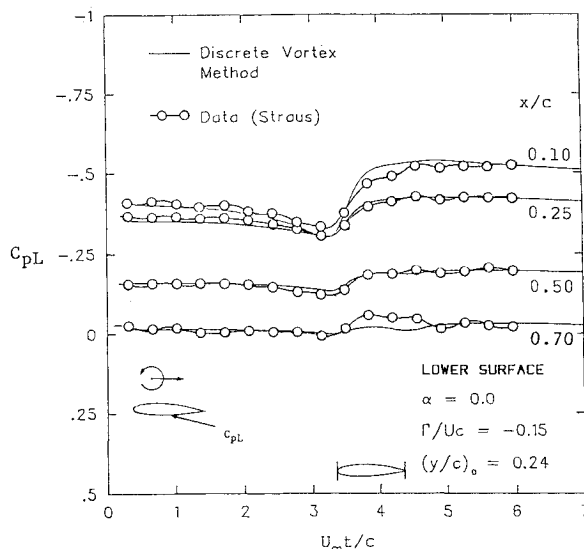


Fig. 10 Measurements of pressure-time history for lower surface and comparisons with theory, $\Gamma/Uc = -0.15$.

The entire pressure-field-time history for the upper and lower surfaces of the test airfoil is shown in Fig. 11. The $t=0$ plane shows the initial steady-state pressure distribution over the airfoil. The increase in lift as a result of the vortex interaction is clearly evident as the pressure on the upper surface decreases, whereas the pressure is seen to increase on the lower surface. The strongest effects of the interaction are confined to the leading-edge region as was already observed by other investigators.^{21,22-25}

Integration of the measured pressure-time-history results

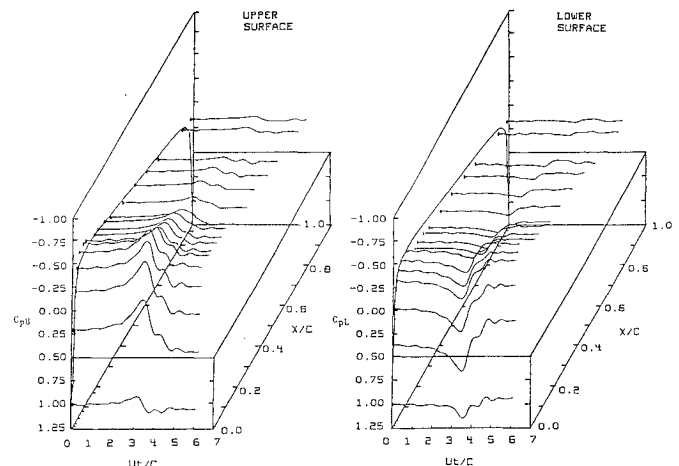


Fig. 11 Temporal pressure distribution on airfoil, $\Gamma/Uc = -0.15$.

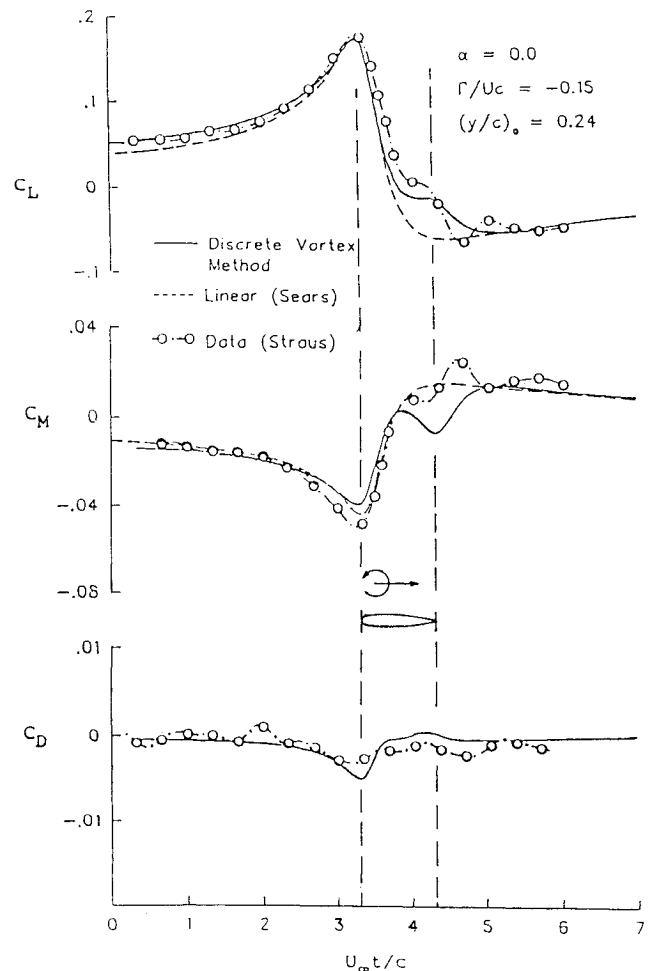


Fig. 12 Temporal variation in lift, moment, and drag coefficients, $\Gamma/Uc = -0.15$.

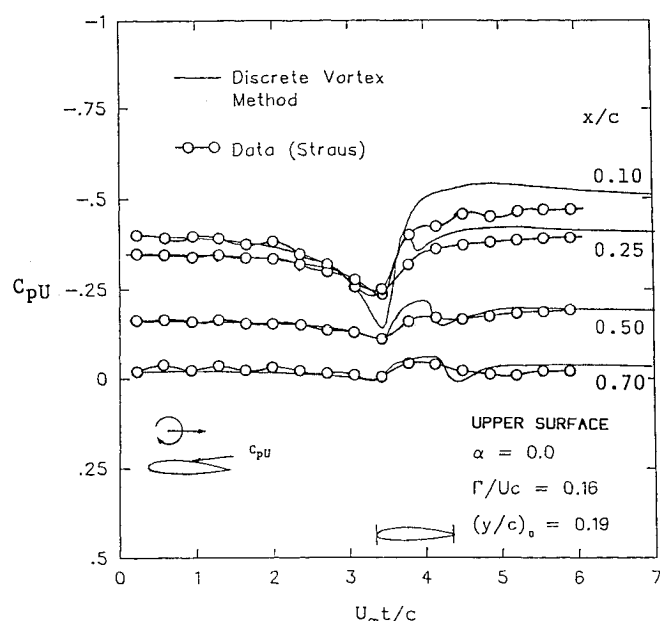


Fig. 13 Measurements of pressure-time history for upper surface and comparison with theory, $\Gamma/Uc=0.16$.

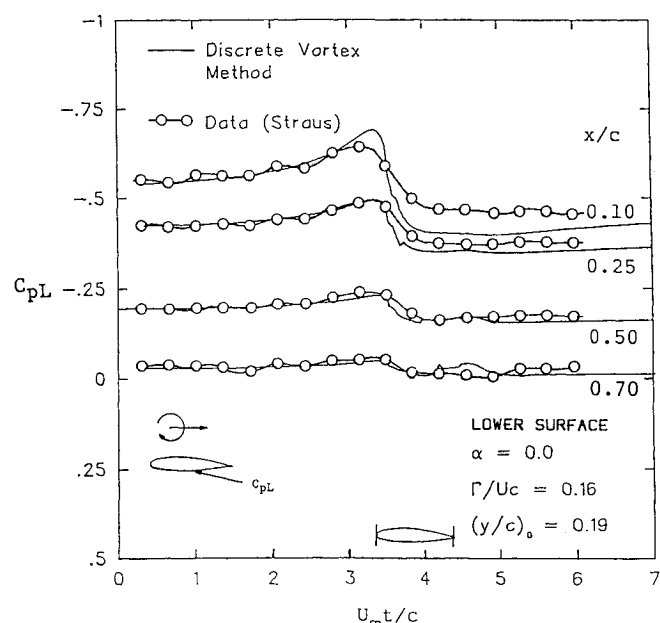


Fig. 14 Measurements of pressure-time history for lower surface and comparison with theory, $\Gamma/Uc=0.16$.

such as those shown in Fig. 11 provides the lift, moment, and drag information during a blade-vortex interaction. These results are shown in Fig. 12, where the lift, moment, and drag coefficients, respectively, are plotted against time and compared to theory. The trend of the results is not unexpected. Initially, the lift increases and the moment (positive clockwise about the leading edge) decreases as the vortex interacts to produce an incident flow at a higher angle of attack. The behavior then reverses as the vortex leaves the trailing edge. The discrete-vortex method compares very well with the experimental lift. As the vortex goes by, the trailing edges both show the same behavior. The linear result of Sears, however, shows a distinctly different behavior in the trailing edge. This is also seen in the temporal variation of the moment coefficient. In this case, however, neither theory agrees as well as the lift comparison. Again, the largest discrepancy is in the trailing-edge region. The theory and data compare well for the

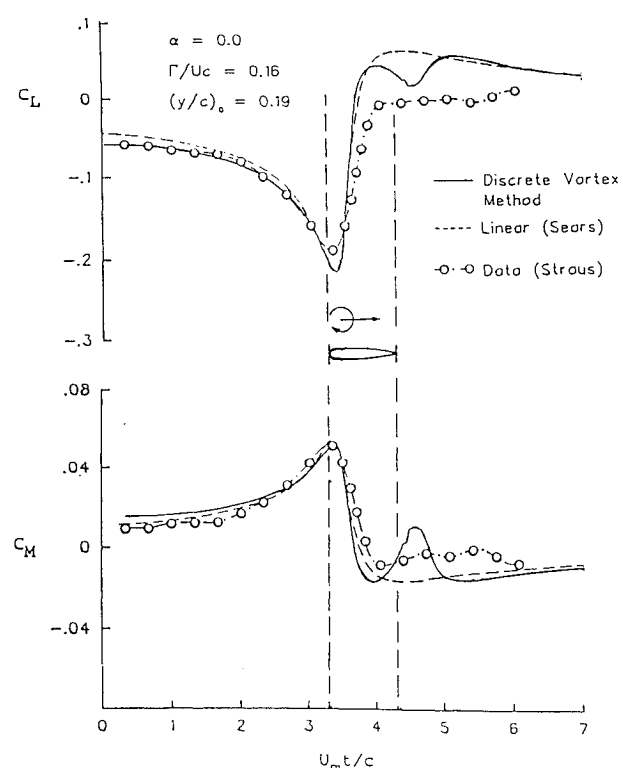


Fig. 15 Temporal variation of the lift and moment coefficients, $\Gamma/Uc=0.16$.

drag coefficient, although too few pressure taps are perhaps available to determine an accurate experimental result.

The results for an interaction where a vortex with a clockwise circulation of $\Gamma/Uc=0.16$ passed about one-fifth of a chord above the airfoil is shown in Figs. 13–15. Figures 13 and 14 show the temporal pressure variations at several chordwise locations. In this case, the agreement between the data and theory is good only up to the leading edge, after which they agree only at the aft chordwise positions. The discrepancy in the pressures is seen dramatically in the temporal lift and moment variations shown in Fig. 15. As the vortex approaches the leading edge, the data follow both theories closely. Past the leading edge, however, when the vortex is over the aft portion of the airfoil, the data diverge from theory until both the lift and moment suddenly level off.

The failure of both theories to predict the observed behavior for the clockwise vortex interaction raises a number of concerns, particularly since it is the situation that an advancing helicopter blade would encounter on a powered descent. The observed discrepancy appears to be a result of flow separation over the suction side of the airfoil, which neither theory presently takes into account. This point is supported by the sudden leveling off of the lift and moment. Also, for the clockwise rotating vortex, the interaction retards the flow on the upper surface. A careful examination of the results from the experiments for both the clockwise and counterclockwise vortex indicates that the region of favorable pressure gradient near the leading edge decreases for the clockwise vortex interactions and increases for the other. Considering that the chordwise Reynolds number of the flow is about 375,000 for the present results, separation on the airfoil is quite possible. It should be pointed out, however, that boundary-layer measurements in steady flow, both with and without a small trip wire attached near the leading edge of the test airfoil, showed that a turbulent boundary layer existed over the airfoil, even without the trip. Therefore, if separation occurs, it either occurs very early on the leading edge as a laminar separation or further aft as a turbulent separation. Of course, more detailed measurements of the flow are required before a more definitive statement can be made.

Conclusions

The present experiments indicate that the pressure on an airfoil during its interaction with a vortex can be predicted only sometimes by inviscid theories. It appears that the situations where an inviscid theory is adequate are either when the vortex passes far away from the airfoil or when the direction of the vortex is such as to accelerate the flow on the facing airfoil surface. Although not fully confirmed, it also appears that a blade-vortex interaction, which tends to retard the flow on the facing airfoil surface (the case with the clockwise vortex in the present experiment), can produce a large separation from which the airfoil does not recover until the vortex is well past the trailing edge. If this is true, then a proper viscous-inviscid model is required for any blade-vortex interaction theory. Such models are currently available (see, for example, Wu et al.³⁵ and Srinivasan³⁶) but are quite involved for use in present-day design systems. An alternative and simpler approach in this regard has recently been taken by Renzoni and Mayle.³⁷ Their method uses incremental force and moment coefficients obtained from both theory and experiments which can be used by the designer.

Acknowledgment

This work was sponsored by the Army Research Office through the Rotorcraft Center at Rensselaer Polytechnic Institute under Contract DAAG29-92-K-0093.

References

- ¹Widnall, S., "Helicopter Noise Due to Blade-Vortex Interaction," *Journal of the Acoustical Society of America*, Vol. 50, No. 1, Pt. 2, July 1971, 354-365.
- ²Nakamura, Y., "Prediction of Blade-Vortex Interaction Noise from Measured Blade Pressure Distributions," Seventh European Rotorcraft and Powered Lift Aircraft Forum, 32, Deutsche Gesellschaft für Luft- und Raumfahrt e. V., Paper 32, Vol. 1, Sept. 1981.
- ³Schlinder, R. H. and Amiet, R. K., "Rotor-Vortex Interaction Noise," AIAA Paper 83-0720, 1983.
- ⁴Ahmadi, A. R., "An Experimental Investigation of Blade-Vortex Interaction at Normal Incidence," Workshop on Blade-Vortex Interaction, NASA Ames Research Center, Oct. 1984.
- ⁵Paterson, R. W., Amiet, R. K., and Munch, C. L., "Isolated Airfoil-Tip Vortex Interaction Noise," *Journal of Aircraft*, Vol. 12, No. 3, Jan. 1975, pp. 34-40.
- ⁶Boxwell, D. A., Schmitz, F. H., Spletstoesser, W. R., and Schultz, K. J., "Helicopter Model Rotor-Blade Vortex Interaction Impulsive Noise: Scalability and Parametric Variations," *Journal of the American Helicopter Society*, Vol. 32, Jan. 1987, pp. 3-12.
- ⁷Hubbard, J. E. and Leighton, K. P., "Comparison of Model Helicopter Rotor Primary and Secondary Blade/Vortex Interaction Blade Slap," *Journal of Aircraft*, Vol. 21, May, pp. 346-350.
- ⁸Martin, R. M., Elliot, J. W., and Hoad, D. R., "Experimental and Analytical Predictions of Rotor Blade Vortex Interaction," *Journal of American Helicopter Society*, Oct. 1986, pp. 12-20.
- ⁹Brotherhood, P., "An Appraisal of Rotor Blade-Tip Vortex Interactions and Wake Geometry from Flight Measurements," AGARD CP-334, May 1982.
- ¹⁰Schmitz, F. H., Boxwell, D. A., Lewy, S., and Dahan, C., "Model- to Full-Scale Comparisons of Helicopter Blade-Vortex Interaction Noise," *Journal of the American Helicopter Society*, April 1984, pp. 16-25.
- ¹¹George, A. R., "Helicopter Noise: State of the Art," *Journal of Aircraft*, Vol. 15, Nov. 1978, pp. 707-715.
- ¹²Schmitz, F. H. and Yu, Y. H., "Helicopter Impulsive Noise: Theoretical and Experimental Status," International Symposium on Recent Advances in Aerodynamics and Aeroacoustics, Stanford Univ., Stanford, CA, Aug. 1983.
- ¹³Ham, N. D., "Some Preliminary Results from an Investigation of Blade-Vortex Interaction," *Journal of the American Helicopter Society*, Vol. 19, No. 2, April 1974, pp. 45-48.
- ¹⁴Ham, N. D., "Some Conclusions from an Investigation of Blade-Vortex Interactions," *Journal of the American Helicopter Society*, Vol. 20, No. 4, Oct. 1975, pp. 26-30.
- ¹⁵Neuwerth, G. and Muller, R., "Pressure Fluctuations on Rotor Blades Generated by Blade-Vortex Interactions," *Vertica*, Vol. 9, No. 3, 1985, pp. 227-239.
- ¹⁶McAlister, K. W. and Tung, C., "Airfoil Interaction with an Impinging Vortex," NASA TP-2273, AVSCOM TR-83-A-17, Feb. 1984.
- ¹⁷Wilson, D. R. and Seath, D. D., "Experimental Simulation of Transonic Vortex-Airfoil Interactions," Workshop on Blade-Vortex Interaction, NASA Ames Research Center, Oct. 1984.
- ¹⁸Surendraiah, M., "An Experimental Study of Rotor Blade-Vortex Interaction," NASA CR-1573, May 1970.
- ¹⁹Caradonna, F. X., Laub, G. H., and Tung, C., "An Experimental Investigation of the Parallel Blade-Vortex Interaction," Workshop on Blade-Vortex Interaction, NASA Ames Research Center, Oct. 1984.
- ²⁰Ziada, S. and Rockwell, D., "Vortex-Leading Edge Interaction," *Journal-Fluid Mechanics*, Vol. 118, 1982, pp. 79-107.
- ²¹Seath, D. D., Jai-Moo, K., and Wilson, D. R., "An Investigation of the Parallel Blade-Vortex Interaction in a Low-Speed Wind Tunnel," AIAA Paper 87-1345, 1987.
- ²²Yu, J. C., "Flow Field Visualization of Two Dimensional Blade-Vortex Interactions," Workshop on Blade-Vortex Interaction, NASA Ames Research Center, Oct. 1984.
- ²³Booth, E. R., and Yu, J. C., "Two Dimensional Blade-Vortex Interaction Flow Visualization Investigation," AIAA Paper 84-2307, 1984.
- ²⁴Booth, E. R. and Yu, J. C., "New Technique for Experimental Generation of Two-Dimensional Blade-Vortex Interaction at Low Reynolds Numbers," NASA TP-2551, March 1986.
- ²⁵Booth, E. R., "Surface Pressure Measurement During Low Speed Two-Dimensional Blade-Vortex Interaction," AIAA Paper 86-1856, 1986.
- ²⁶Meier, G. E. A., Timm, R., and Becker, F., "Initial Experiments on Profile Vortex Interaction," Max Planck Institute für Stromungsforschung, ISSN 0436-1199, June 1983.
- ²⁷Meier, G. E. A. and Timm, R., "Unsteady Vortex Airfoil Interaction," AGARD CP-386, May 1985.
- ²⁸Renzoni, P., "Discrete Vortex Modeling of a Blade-Vortex Interaction," Ph.D. Thesis, Rensselaer Polytechnic Inst., Troy, NY, 1987.
- ²⁹Bergman, R. A., "Design and Performance of a Blade-Vortex Interaction Experiment," M.S. Thesis, Rensselaer Polytechnic Inst., Troy, NY, 1984.
- ³⁰Straus, J., "Airfoil Pressure Measurements for a Two-Dimensional Blade-Vortex Interaction," M.S. Thesis, Rensselaer Polytechnic Inst., Troy, NY, 1986.
- ³¹Theodorsen, T., "General Theory of Aerodynamic Instability and the Mechanism of Flutter," NACA TR-496, 1935.
- ³²Sears, W. R., "Aerodynamics, Noise, and the Sonic Boom," *AIAA Journal*, Vol. 7, April 1969, pp. 577-586.
- ³³Fung, Y. C., "An Introduction to the Theory of Aeroelasticity," Wiley, New York, 1955, Chaps. 6 and 15.
- ³⁴Srinivasan, G. R., McCroskey, W. J., and Baeder, J. D., "Aerodynamics of Two-Dimensional Blade-Vortex Interaction," *AIAA Journal*, Vol. 24, Oct. 1986, pp. 1569-1576.
- ³⁵Wu, J. C., Hsu, T. M., and Sankar, L. H., "Viscous Flow Results for the Vortex-Airfoil Interaction Problem," AIAA Paper 85-4053, 1985.
- ³⁶Srinivasan, G. R., "Computations of Two Dimensional Airfoil-Vortex Interactions," NACA CR-3885, 1985.
- ³⁷Renzoni, P. and Mayle, R. E., "Incremental Force and Moment Coefficients for a Parallel Blade-Vortex Interaction" (submitted for publication in *AIAA Journal*).